

AD A111327

Prepared for
SPACE DIVISION
AIR FORCE SYSTEMS COMMAND
Los Angeles Air Force Station
P.O. Box 98900, Worldway Postal Center
Los Angeles, Calif. 90009

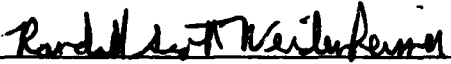
A


8202 24 008
407512

This report was submitted by The Aerospace Corporation, El Segundo, CA 90245, under Contract No. F04701-81-C-0082 with the Space Division, Deputy for Technology, P.O. Box 92960, Worldway Postal Center, Los Angeles, CA 90009. It was reviewed and approved for The Aerospace Corporation by G. A. Paulikas, Director, Space Sciences Laboratory. Lt R. S. Weidenheimer, SD/YLVS, was the project officer for Mission Oriented Investigation and Experimentation (MOIE) Programs.

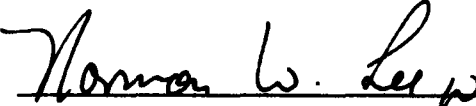
This report has been reviewed by the Public Affairs Office (PAS) and is releasable to the National Technical Information Service (NTIS). At NTIS, it will be available to the general public, including foreign nations.

This technical report has been reviewed and is approved for publication. Publication of this report does not constitute Air Force approval of the report's findings or conclusions. It is published only for the exchange and stimulation of ideas.


Randall S. Weidenheimer, 2nd Lt, USAF
Project Officer


Florian P. Meinhardt, Lt Col, USAF
Director of Advanced Space Development

FOR THE COMMANDER


Norman W. Lee, Jr., Colonel, USAF
Deputy for Technology

UNCLASSIFIED

SECURITY CLASSIFICATION OF THIS PAGE (When Data Entered)

REPORT DOCUMENTATION PAGE		READ INSTRUCTIONS BEFORE COMPLETING FORM
1. REPORT NUMBER SD-TR-81-39	2. GOVT ACCESSION NO. AD-A111 327	3. RECIPIENT'S CATALOG NUMBER
4. TITLE (and Subtitle) ASPECT DEPENDENCE AND FREQUENCY SPECTRUM OF ELECTRICAL DISCHARGES ON THE P78-2(SCATHA) SATELLITE	5. TYPE OF REPORT & PERIOD COVERED	
	6. PERFORMING ORG. REPORT NUMBER TR-0082(2940-06)-3	
7. AUTHOR(s) Harry C. Koons	8. CONTRACT OR GRANT NUMBER(s) F04701-81-C-0082	
9. PERFORMING ORGANIZATION NAME AND ADDRESS The Aerospace Corporation El Segundo, Calif. 90245	10. PROGRAM ELEMENT, PROJECT, TASK AREA & WORK UNIT NUMBERS	
11. CONTROLLING OFFICE NAME AND ADDRESS Space Division Air Force Systems Command Los Angeles, Calif. 90009	12. REPORT DATE 15 January 1982	
	13. NUMBER OF PAGES 30	
14. MONITORING AGENCY NAME & ADDRESS (if different from Controlling Office)	15. SECURITY CLASS. (of this report) Unclassified	
	15a. DECLASSIFICATION/DOWNGRADING SCHEDULE	
16. DISTRIBUTION STATEMENT (of this Report) Approved for public release; distribution unlimited		
17. DISTRIBUTION STATEMENT (of the abstract entered in Block 20, if different from Report)		
18. SUPPLEMENTARY NOTES		
19. KEY WORDS (Continue on reverse side if necessary and identify by block number) Electrical Discharges Pulse Analyzer Spacecraft Charging		
20. ABSTRACT (Continue on reverse side if necessary and identify by block number) The SCATHA (P78-2) satellite payload includes a Charging Electrical Effects Analyzer to measure the characteristics of electrical discharges that occur on the vehicle due to spacecraft charging. During 233 days of operation, 19 pulses on 10 different days have been related to electrical discharges. Five of these discharges took place when the pulse analyzer was in a mode with sufficient time resolution to resolve the frequency components in the waveform. The dominant frequencies ranged from 5 to 32 MHz with amplitudes from 0.4 to 0.9 V into a 50-ohm load.		

DD FORM 1473
(FACSIMILE)

UNCLASSIFIED
SECURITY CLASSIFICATION OF THIS PAGE (When Data Entered)

CONTENTS

SUMMARY..... 7
INTRODUCTION..... 7
INSTRUMENT DESCRIPTION..... 8
DATA..... 10
NATURAL CHARGING EVENTS..... 12
ASPECT DEPENDENCE..... 20
FREQUENCY SPECTRUM..... 20
REFERENCES..... 29

Accession For
NTIS GRAS
DTIC TAB
Unannounced
Justification

A



TABLES

1.	Pulse Analyzer Settings.....	11
2.	Distribution of Pulses Detected by the Pulse Analyzer.....	13
3.	Summary of Discharges.....	14
4.	Solar Direction in Satellite Coordinates at Time of Pulse.....	21
5.	Natural Discharge Fitting Parameters.....	24
6.	Pulse Fitting Parameters.....	27

RECORDING PAGE BLANK-NOT FILMED

FIGURES

1.	Functional Block Diagram of the SC1-8B Pulse Analyzer.....	9
2.	Summary of the Charging Event in Eclipse on 28 March 1979.....	15
3.	Differential Voltage of a Surface Potential Monitor, Kapton Sample to Space Vehicle Ground.....	17
4.	Amplitude Distribution of the 19 Natural Discharges Detected by the Pulse Analyzer.....	18
5.	Local Time Distribution of the 19 Natural Discharges Detected by the Pulse Analyzer.....	19
6.	Direction of the Sun in Space Vehicle Coordinate System When Natural Discharges Occurred.....	22
7.	Shape of Three Natural Discharges Detected by the Pulse Analyzer.....	25
8.	Shape of Two Natural Discharges Detected by the Pulse Analyzer.....	26
9.	Shape of Two Pulses Due to Vehicle Operations.....	28

INSTRUCTIONS PAGE BLANK-NOT FILLED

SUMMARY

The SCATHA (P78-2) satellite payload includes a Charging Electrical Effects Analyzer (CEEA) to measure the characteristics of electrical discharges in both the frequency and time domain. Pulses are detected in response to commands, during electron and ion beam operations and during natural discharge events. The Pulse Analyzer which measures the shape of pulses on four sensors is the primary CEEA diagnostic for the natural discharges. To date 233 days of Pulse Analyzer data have been reduced. Nineteen pulses on ten different days have been related to natural discharges. Many of these are related to the solar illumination of the vehicle. Two occurred shortly after the satellite exited the earth's umbra. On May 26, 1979 six pulses were detected in sunlight within a period of 14 minutes. All six occurred at precisely the same spin phase suggesting that a single point on the vehicle was breaking down. Only five discharges have been found in the data at a time when the Pulse Analyzer was in mode with sufficient time resolution to resolve the frequency components in the waveform.

INTRODUCTION

The Charging Electrical Effects Analyzer (CEEA) was provided for the SCATHA (P78-2) satellite payload to verify that electrical discharges are occurring when other instruments measure large differential potentials between surface materials on the vehicle.

*This work was supported by the U. S. Air Force under Contract No. F04701-80-C-0081.

The CEEA consists of three instruments: the Pulse Analyzer, the VLF Analyzer, and the RF Analyzer. The Pulse Analyzer measures the number of pulses, their amplitudes and shapes on four sensors. The VLF Analyzer measures the electric and magnetic field spectra of waves in the frequency range from 100 Hz to 300 kHz. The RF Analyzer measures the electric field intensity on a 1.8-m monopole antenna in the frequency range from 2 to 30 MHz.

In this paper I present results from the Pulse Analyzer from 233 days between 7 February 1979 and 20 June 1980. This period covers quiet and active days, eclipses, and electron and ion beam operations. The instrument is described in the next section. That is followed by a presentation of the statistics of pulses detected. Individual time periods of special interest are described in detail. In the final sections the aspect dependence and frequency spectrum of the natural discharges are described.

INSTRUMENT DESCRIPTION

The Pulse Analyzer measures the shape of electromagnetic pulses in the time domain from 7 ns to 3.7 ms. The pulse analyses are made on four sensors: (1) a loop antenna around one of the two redundant space vehicle Command Distribution Units, (2) a wire along the outside of a "typical" space vehicle cable bundle, (3) an external short dipole antenna at the end of a 2-m boom, and (4) a digital command line from the Command Distribution Unit to the Pulse Analyzer.

The signal processor may be switched by command to any of the four sensors. It then steps automatically through the selected sensors monitoring each in turn for 16 sec. The functional block diagram is shown in Figure 1. When a signal exceeds a commandable threshold its amplitude is sampled at 16 points to measure the pulse shape. The 16 samples may be spaced logarithmically or linearly in time. The logarithmic spacing covers the range from 7 ns to 492 μ s. The linear spacing is commandable with the following options: 0.015, 0.060, 0.24, 1.0, 3.8, 30, and 250 μ s. The amplitude is measured by a bank of 24 discriminators, 12 positive and 12 negative. The total range of the discriminator bank is 3 mV to 1.8 V. The signal from each sensor can be

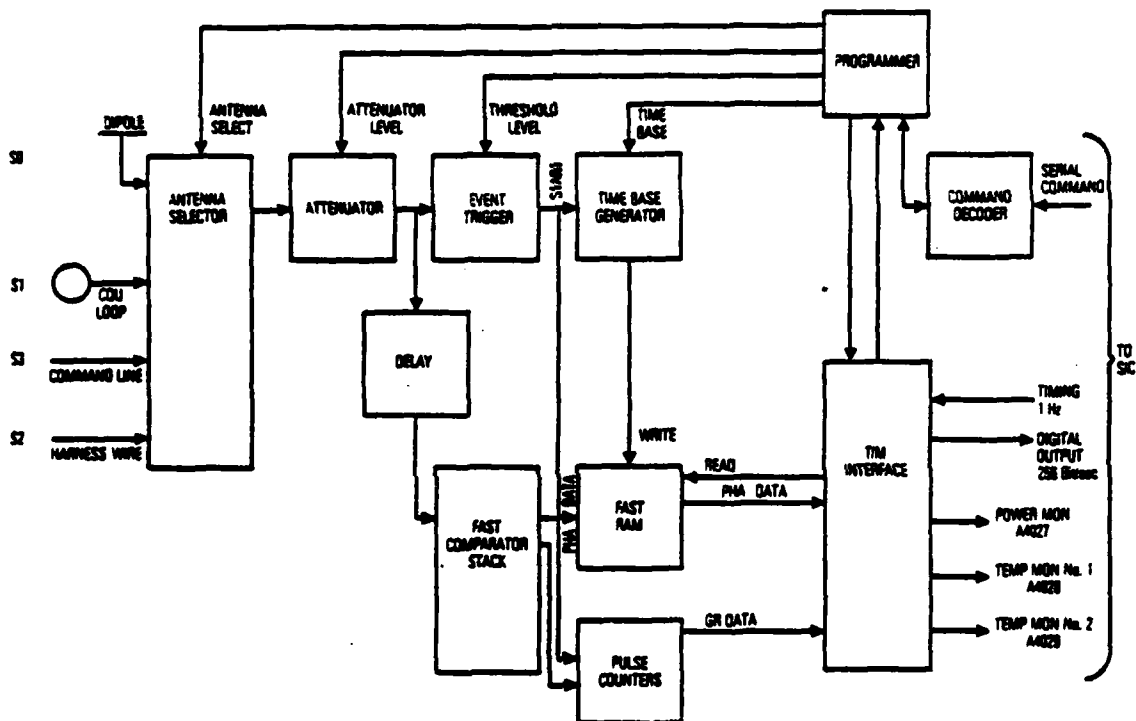


Figure 1. Functional Block Diagram of the SCI-8B Pulse Analyzer

attenuated by command to place it within this range. There are six attenuation settings that select measurement ranges from 3 mV to 1.84 V at minimum attenuation to 3.46 V to 1910 V at maximum attenuation. The threshold is coupled to the attenuation setting. The attenuation, threshold, and sampling interval can be independently commanded for each sensor. The number of pulses per second above four selectable thresholds is also measured. Three of the thresholds are determined by the attenuation selection, the fourth is the pulse analysis threshold.

The instrument is commanded by a 22-bit serial magnitude command of which only the seven least significant bits are used.

In its normal mode of operation the instrument steps through each of four sensors monitoring each for 16 sec in sequence. The threshold and attenuations for each sensor are determined by experience on orbit.

Initial measurements have been made with the logarithmic sample spacing. Linear spacing (15 ns) has been used since October 1979 because typical pulses prove to be shorter than 200 ns.

Inflight verification of the calibration is accomplished by sending serial magnitude commands from the Command Distribution Unit to the serial magnitude command sensor.

DATA

The Pulse Analyzer was turned-on and successfully checked out on-orbit on February 5, 1979. Initial operations began with the pulse analysis threshold set at 0.651 V and the countrate thresholds set as shown in table 1, column 1. At this setting only two pulses were detected during the 72 hours of data available from February 12-14. Both of these pulses occurred during SC4-2 Ion Beam operations on February 14. The pulses had a width at half maximum of 500 μ s and an amplitude of 0.7 V.

Because it was apparent that very few pulses were being detected the threshold was lowered on February 18 to 0.165 V with the associated countrate thresholds listed in table 1, column 2.

Table 1

PULSE ANALYZER SETTINGS

THRESHOLDS	TIME PERIOD			
	2/ 5/79 - 2/17/79	2/18/79 - 4/26/79	4/27/79 - 10/11/79	10/11/79 - 3/14/80
Pulse Analysis, volts	0.651	0.165	0.327	0.327
Countrate CR0, volts	0.117	0.030	0.117	0.030
Countrate CR1, volts	1.85	0.469	1.85	0.469
Countrate CR2, volts	28.3	7.18	28.3	7.18
Countrate CR3, volts	0.651	0.165	0.327	0.165
Pulse Analysis Range, volts	0.05-29.2	0.014-7.43	0.05-29.2	0.05-29.2
Time State	Log	Log	Log	Linear(15ns)

At this threshold the analyzer occasionally responds to pulses generated when commands are sent to the vehicle. Pulses occurring within one second of a command are attributed to a vehicle or payload response to the command and are identified as Command Pulses in table 2.

An interesting variation to this is a pulse that occurs approximately 20 s after the vehicle transmitter is turned off. These have been identified with the time that the ground station command transmitter ceases sending s-tones to the vehicle. They are identified as Command Pulses in table 2.

A second source of pulses is the antenna switch in the VLF Analyzer. This experiment is housed in the same package as the Pulse Analyzer. When the VLF antenna switches from the magnetic antenna to the electric antenna a pulse is detected on the Pulse Analyzer Command Line Sensor. This pulse occurs once every 64 s. Since pulses are synchronized to the vehicle clock they can be readily identified and they have been eliminated from the distributions in table 2.

The majority of the remaining pulses listed in table 2 occur during the electron and ion beam operations.

NATURAL CHARGING EVENTS

Only 19 of the 2557 pulses cannot be associated with normal vehicle commands or ion and electron beam operations. A summary of these pulses is shown in table 3. Some of these pulses occurred during natural charging events that have been studied in detail.

On 28 March, a natural charging event occurred during eclipse. This event was unusual in that the satellite was in the earth's shadow over 1000 s before an injection of hot plasma near local midnight charged the vehicle negatively. Figure 2 shows a composite of data from the Satellite Surface Potential Monitors (SSPM), the Pulse Analyzer, and the electron and ion detectors on the Sheath Electric Field Experiment (SEFE). The SSPM and SEFE instruments are described in reference 1. The differential potential between a Kapton sample and the vehicle frame is plotted as a function of time in the bottom panel. At the time the Kapton potential abruptly increases from back-

Table 2
 DISTRIBUTION OF PULSES DETECTED
 BY THE PULSE ANALYZER

MONTH	DAYS	<u>THRESHOLD</u> VOLTS	TOTAL PULSES	COMMAND PULSES	ELECTRON BEAM PULSES	ION BEAM PULSES	DIS- CHARGE PULSES
79 FEB	10	0.65	15	6	0	9	0
	11	0.17	66	66	-	-	0
MAR	25	0.17	519	249	175	93	2
APR	25	0.17	660	349	10	299	2
	4	0.33	48	47	-	-	1
MAY	30	0.33	238	232	-	-	6
JUN	26	0.33	328	180	148	-	0
JUL	5	0.33	33	28	-	5	0
AUG	9	0.33	46	45	-	-	1
SEP	5	0.33	34	33	-	-	1
OCT	7	0.33	74	41	33	-	0
NOV	22	0.33	134	134	-	-	0
DEC	31	0.33	219	219	-	-	0
80 JAN	17	0.33	101	100	-	-	1
APR	1	0.17	1	0	-	-	1
JUN	6	0.17	41	37	-	-	4
TOTAL	234		2557	1766	366	406	19

Table 3
SUMMARY OF DISCHARGES

DATE	UT SECONDS	LOCAL TIME		RADIUS		KAPTON POTENTIAL		COMMENTS
		HOURS		EARTH RADII		VOLTS		
28 MAR 79	59851	23.8		6.3		-1725		ELECTRON INJECTION UMBRALE EXIT + 50 SEC ECLIPSE
28 MAR 79	62088	0.4		6.5		-1689		
14 APR 79	39940	0.2		6.7		-400		
18 APR 79	82767	10.8		6.3		NONE		ONE SAMPLE # 0 (0.2v)
30 APR 79	25616	1.2		7.4		-840		
26 MAY 79	02641	2.6		7.8		-1098		SAME SPIN PHASE
26 MAY 79	02756	2.7		7.8		-1049		
26 MAY 79	02928	2.7		7.8		-1074		
26 MAY 79	03158	2.7		7.8		-1061		
26 MAY 79	03387	2.8		7.8		-1012		
26 MAY 79	03444	2.8		7.8		-1061		
9 AUG 79	02095	2.3		6.7				
18 SEP 79	35981	1.5		6.2				
24 JAN 80	03082							UMBRALE EXIT + 92 SEC
16 APR 80	22281	0.5		7.2				
13 JUN 80	04322	14.0		5.3				
13 JUN 80	06750	15.0		5.6				
14 JUN 80	09770	16.7		5.6				
20 JUN 80	20132	21.6		7.2				

P78-2 Charging Event in Eclipse

28 MARCH 1979

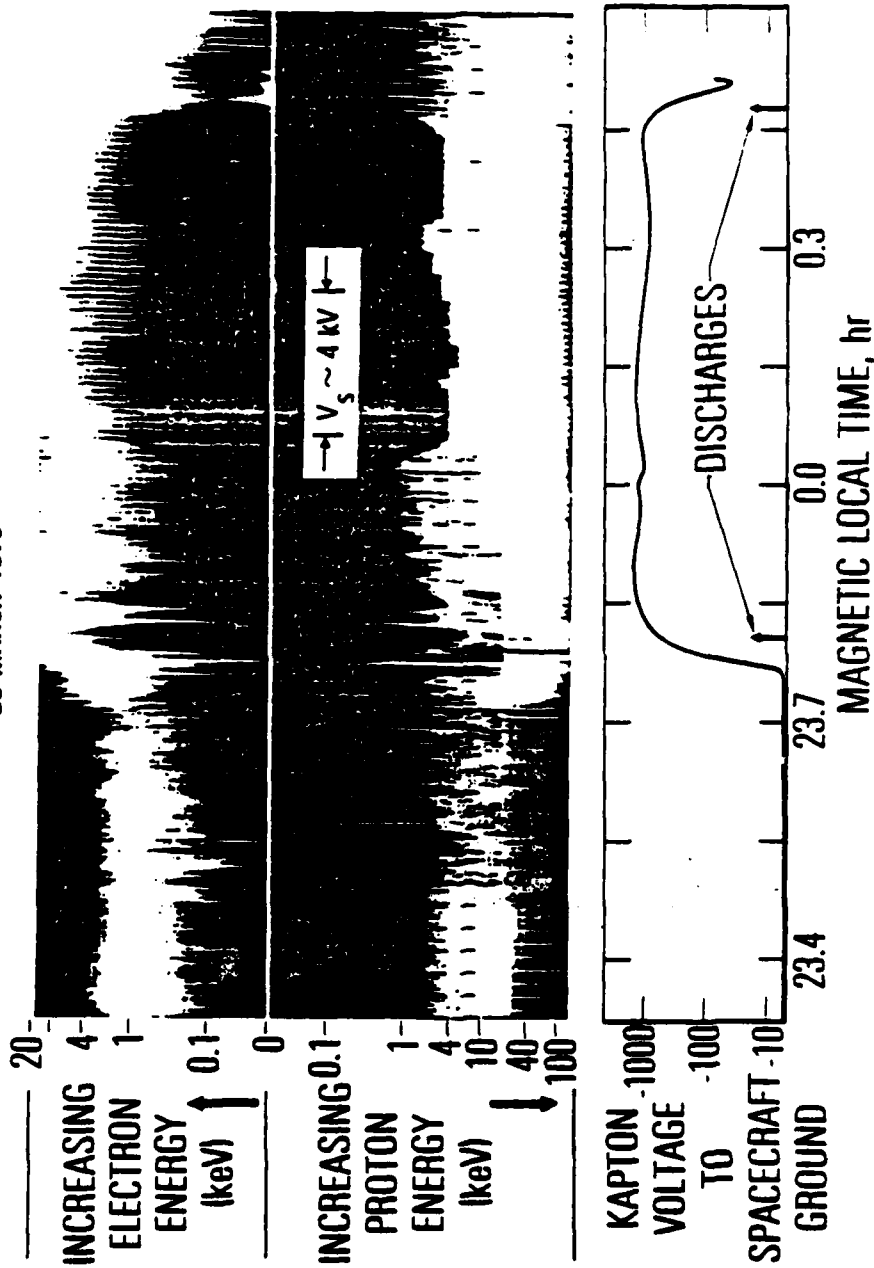


FIGURE 2

Figure 2. Summary of the Charging Event in Eclipse on 28 March 1979. (Top) Electron spectrogram. Increasing lightness corresponds with increasing particle flux. (Middle) Ion spectrogram. (Bottom) Differential voltage of a surface potential monitor, Kapton sample to space vehicle ground. The times of two discharges detected by the pulse analyzer are also indicated.

ground to over one kilovolt, the mean electron energy increases from about one kilovolt to greater than 20 kilovolts. About five minutes later a discharge was detected by the Pulse Analyzer. Later a second discharge and a decrease in the average Kapton potential occurs as the satellite crossed the terminator from shadow into sunlight. During this charging event, the vehicle frame increased to ~ -8000 volts and maintained a potential near -4000 volts until the spacecraft entered the sunlight. The data in figure 2 confirm that the spacecraft charging induced by energetic electrons produced significant differential potentials and electrical discharges. The low energy limit of the protons in figure 2 represents the potential of the spacecraft frame relative to the plasma environment. This is seen to fluctuate around ~ -4 kV during the charging event. The potential between the Kapton sample and the plasma is found by adding the -4 kV of the spacecraft frame to the Kapton voltage.

On May 26, 1979 a series of six pulses was detected by the Pulse Analyzer while the vehicle was in sunlight. These pulses occurred during the enhancement of the differential potential of a Kapton sample on the SSPM on the end of the vehicle (Fig. 3). At that time the spin axis of the vehicle made an angle of 90 deg with the sun-satellite line. At that angle the Kapton sample is shadowed by the vehicle and is not discharged by sunlight. The data from March 28 and May 26 demonstrate the correlation of eight of the 19 pulses with differential charging on the vehicle. These pulses are assumed to be discharges. These pulses were undersampled in the logarithmic time spacing mode being used at the time. Hence frequency information cannot be obtained from them.

Most of the remaining pulses occurred during time periods when the Kapton samples on the Satellite Surface Potential Monitors were charged. The amplitude distribution of the discharges is shown in figure 4. The location of the satellite at the time these pulses occurred is shown in figure 5 as a function of local time and radial distance. This distribution is certainly consistent with the local time dependence of circuit upsets on DoD and commercial satellites (ref. 2). The data from June 1980 plotted at afternoon local times in figure 5 demonstrate that discharges can also occur on the day side of the earth following moderate substorms.

26 MAY 1978

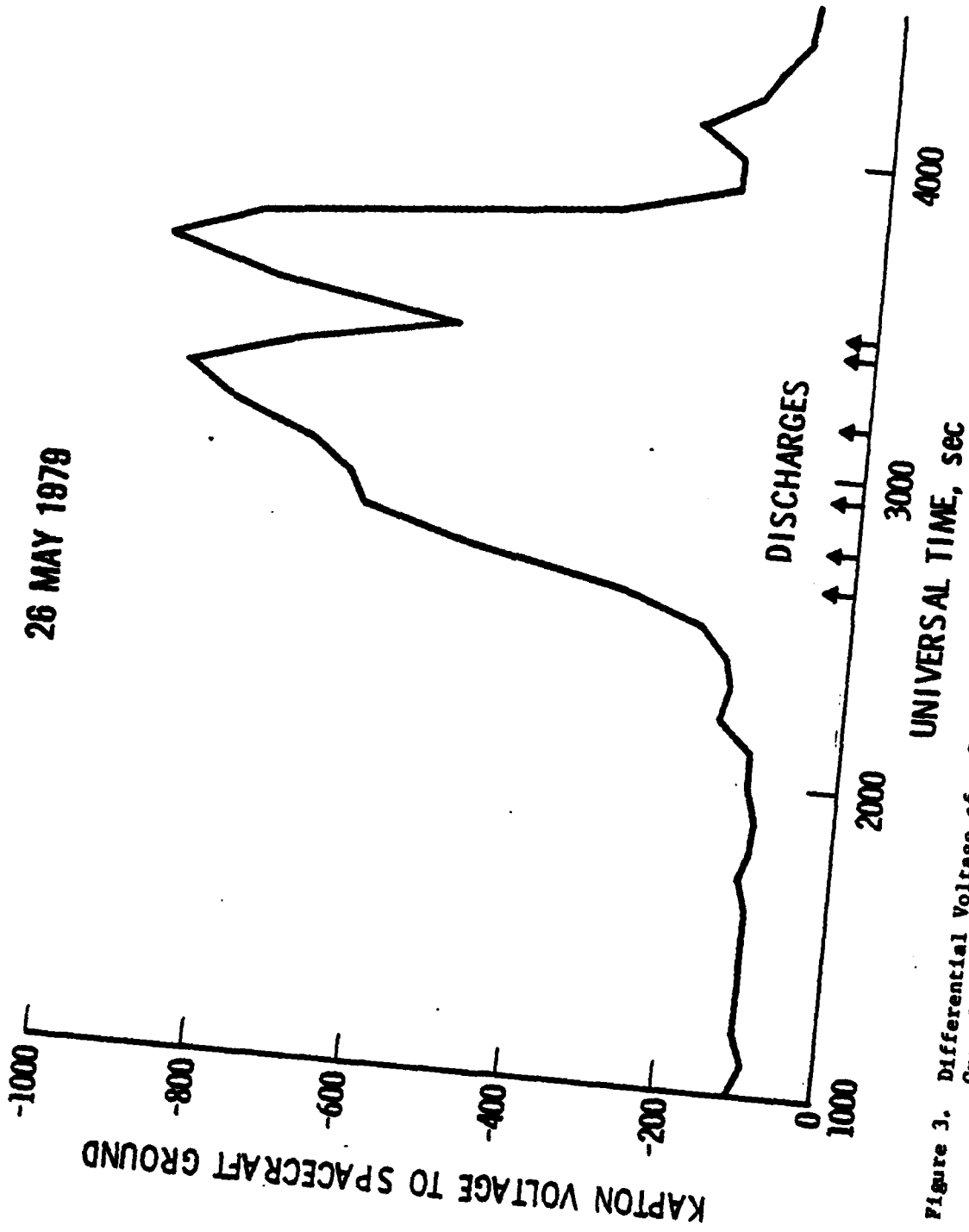


Figure 3. Differential Voltage of a Surface Potential Monitor, Kapton Sample to Space Vehicle Ground. Times of six discharges detected by the pulse analyzer are also indicated.

N = 19

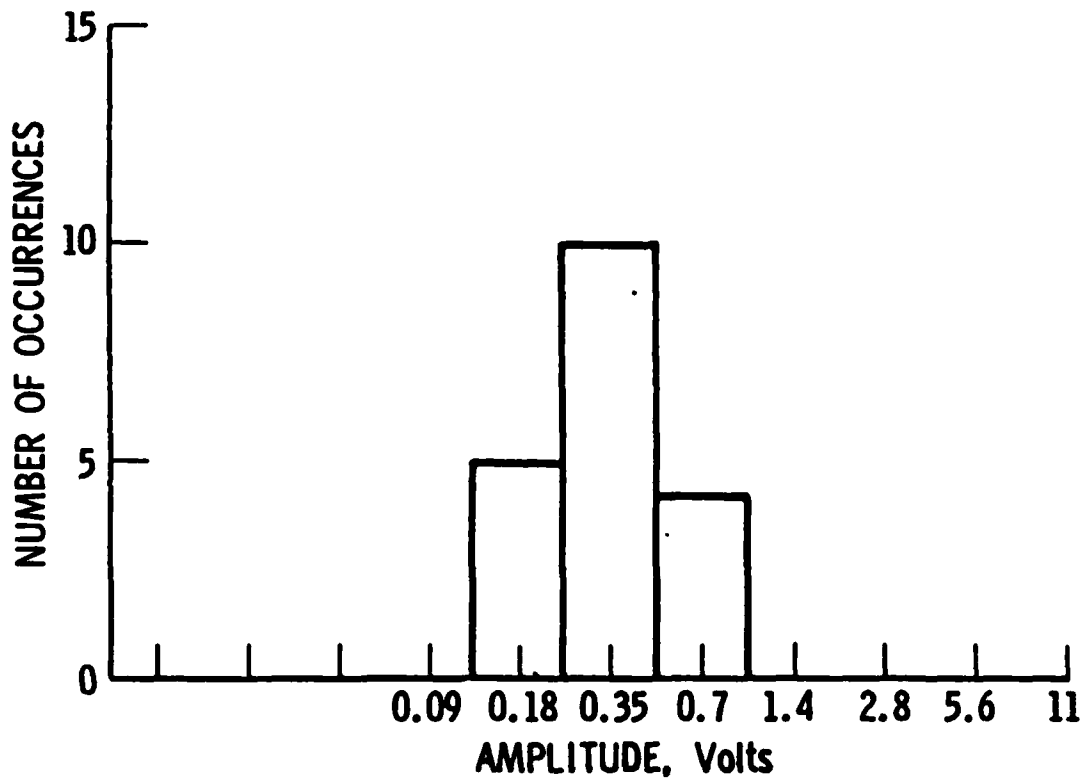


Figure 4. Amplitude Distribution of the 19 Natural Discharges Detected by the Pulse Analyzer

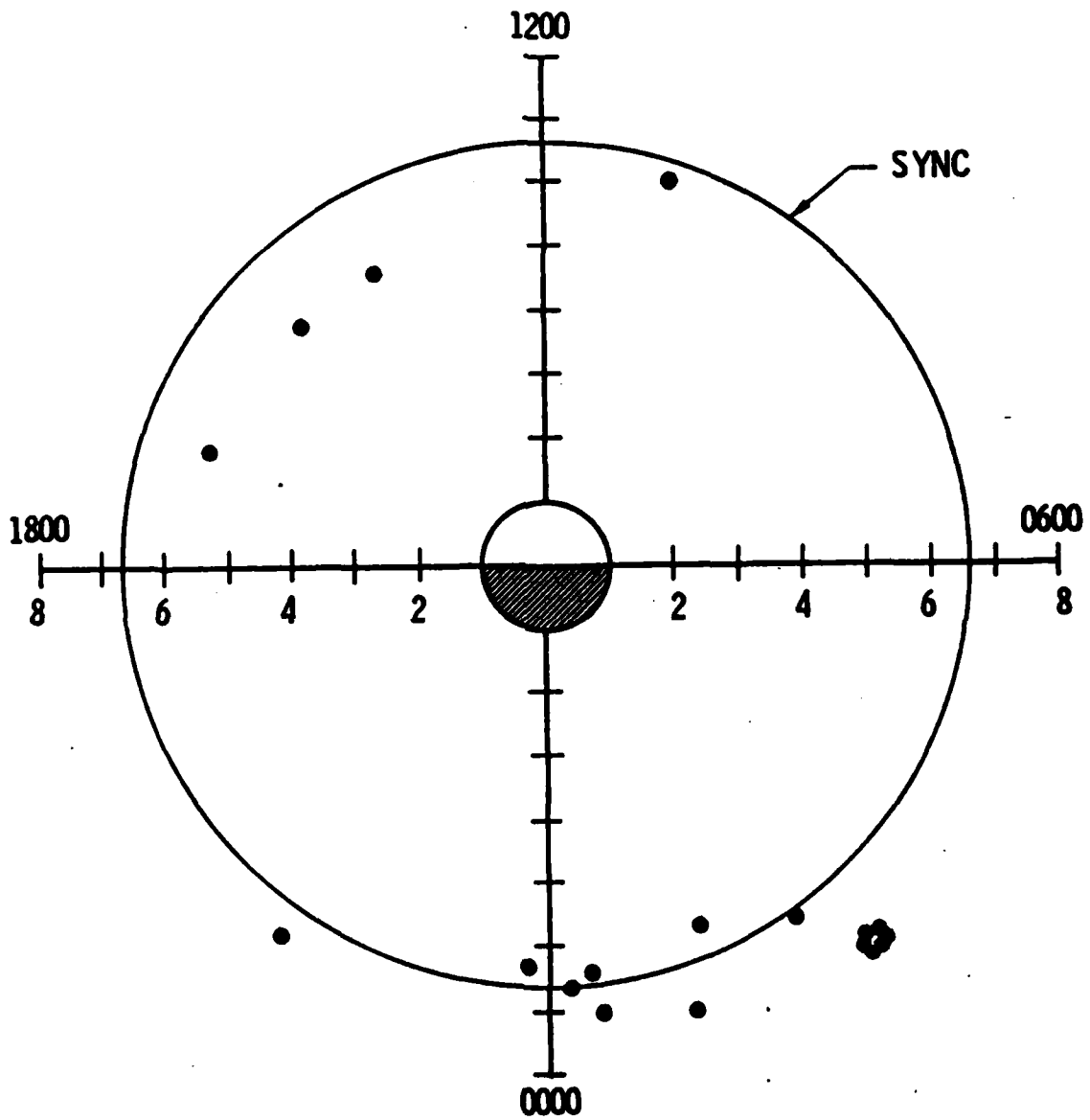


Figure 5. Local Time Distribution of the 19 Natural Discharges Detected by the Pulse Analyzer

The Boulder Geomagnetic Substorm Log lists a moderate substorm at 0745 UT on June 11, and a second onset at 2230 UT on June 11 followed by minor magnetic storm conditions throughout the day on June 12 and 13.

ASPECT DEPENDENCE

The six discharges detected on May 26 occurred at the same rotational phase of the vehicle. Since the vehicle was in sunlight this suggests that one location on the vehicle was arcing. Presumably this would occur when the potential difference suddenly increased as material on one side of the arc was discharged by photocurrent as it passed into sunlight.

In order to determine if discharges on other dates occurred at the same rotational phase the azimuth and elevation of the sun in spacecraft coordinates was calculated for a number of other discharges. The results are tabulated in table 4 and the direction to the sun for these discharges is shown on a schematic of the vehicle in figure 6. There is a large scatter in the data implying that the location and mechanism described above for the May 26 discharges are not the same for the others. The sun does tend to be 180 deg from the magnetometer boom suggesting that this boom plays a role in a significant number of the discharges. NASCAP models of the SCATHA satellite show the largest differential potentials occur at the booms (N. John Stevens, private communication, 1980).

FREQUENCY SPECTRUM

Five discharge pulses have been detected with the pulse analyzer in a mode of operation with a linear sample spacing of 15 nanoseconds. It can then be used to measure the dominant frequency components in each pulse. A computer fit of the functional form

$$V = V_0 + \sum V_1 e^{-k_1 t} \cos(2\pi f_1 t + \phi_1)$$

Table 4
 SOLAR DIRECTION
 IN SATELLITE COORDINATES
 AT TIME OF PULSE

DATE	UT	ELEVATION	AZIMUTH *
	SECONDS	DEG	DEG
28 MAR 79	59851	90.7	19.4
28 MAR 79	62088	90.7	12.6
14 APR 79	39940	84.7	91.5
18 APR 79	82767	88.7	307.9
30 APR 79	25616	87.2	287.2
26 MAY 79	02641	90.3	265.4
26 MAY 79	02756	90.3	263.8
26 MAY 79	02928	90.3	264.5
26 MAY 79	03158	90.3	261.3
26 MAY 79	03387	90.3	264.3
26 MAY 79	03444	90.3	266.6
9 AUG 79	02095	86.0	51.5

*Measured counterclockwise from +z axis in spacecraft coordinate system.

was made to the sixteen sample points. The parameters giving the best fit in the least squares sense are shown in table 5. For highly damped waveforms a decaying exponential term was also included in the sum. The data and fits are shown in figures 7 and 8. The pulses are quite different with dominant frequencies from 5 to 32 MHz and peak amplitudes from 0.08 to 0.89 volts.

To date too few natural discharge pulses have been found to adequately characterize the discharges for the purpose of validating discharge coupling models and ground-based discharge tests using scale-sized models of the SCATHA satellite.

Pulses are also detected during normal vehicle operations and electron and ion beam operations.

On March 23, 1980, the Pulse Analyzer detected a pulse at 1411:36 UT during electron beam operations at 1.5 kV 1 ma. At 1424:20 UT a pulse due to the automatic antenna switch in the VLF experiment was detected. Both pulses were measured on the command sensor line in the high resolution mode. A computer fit was made to the pulse shapes of these pulses in order to compare them with the discharge related pulses. The parameters giving the best fit are shown in table 6.

For the pulse during electron gun operations that best fit was obtained for two frequencies. One of the two frequencies showed a slight growth rate while the other was slightly damped. The pulse shape is shown in figure 9. I believe that the appropriate conclusion is that the damping is very small and that the data set is too short to determine the damping coefficient.

For the antenna switch pulse the best fit was again obtained for two frequencies. The frequencies differ significantly from those obtained for the electron beam pulse and the natural discharges. The antenna switch pulse is shown in figure 9.

Table 5
 NATURAL DISCHARGE FITTING PARAMETERS

Date	UT Seconds	Sensor	i	Frequency MHz	Amplitude volts	Damping ns^{-1}	Phase deg
1/24/80	03082	CMD	0		0.01		
			1	5.0	0.38	3.4×10^{-4}	112
			2	25.7	0.13	1.5×10^{-2}	-3
4/16/80	22281	Dipole	0		0.00		
			1	11.1	0.89	2.2×10^{-2}	29
			2	25.0	0.68	7.7×10^{-3}	173
6/13/80	06750	Harness	0		0.08		
			1	19.5	0.25	9.4×10^{-3}	175
			2	31.8	0.80	6.3×10^{-3}	-66
6/14/80	09770	Dipole	0		0.00		
			1	13.3	0.06	1.6×10^{-2}	103
			2	26.1	0.08	2.5×10^{-2}	79
6/20/80	20132	Dipole	0		0.24		
			1	21.7	0.12	6.9×10^{-2}	21

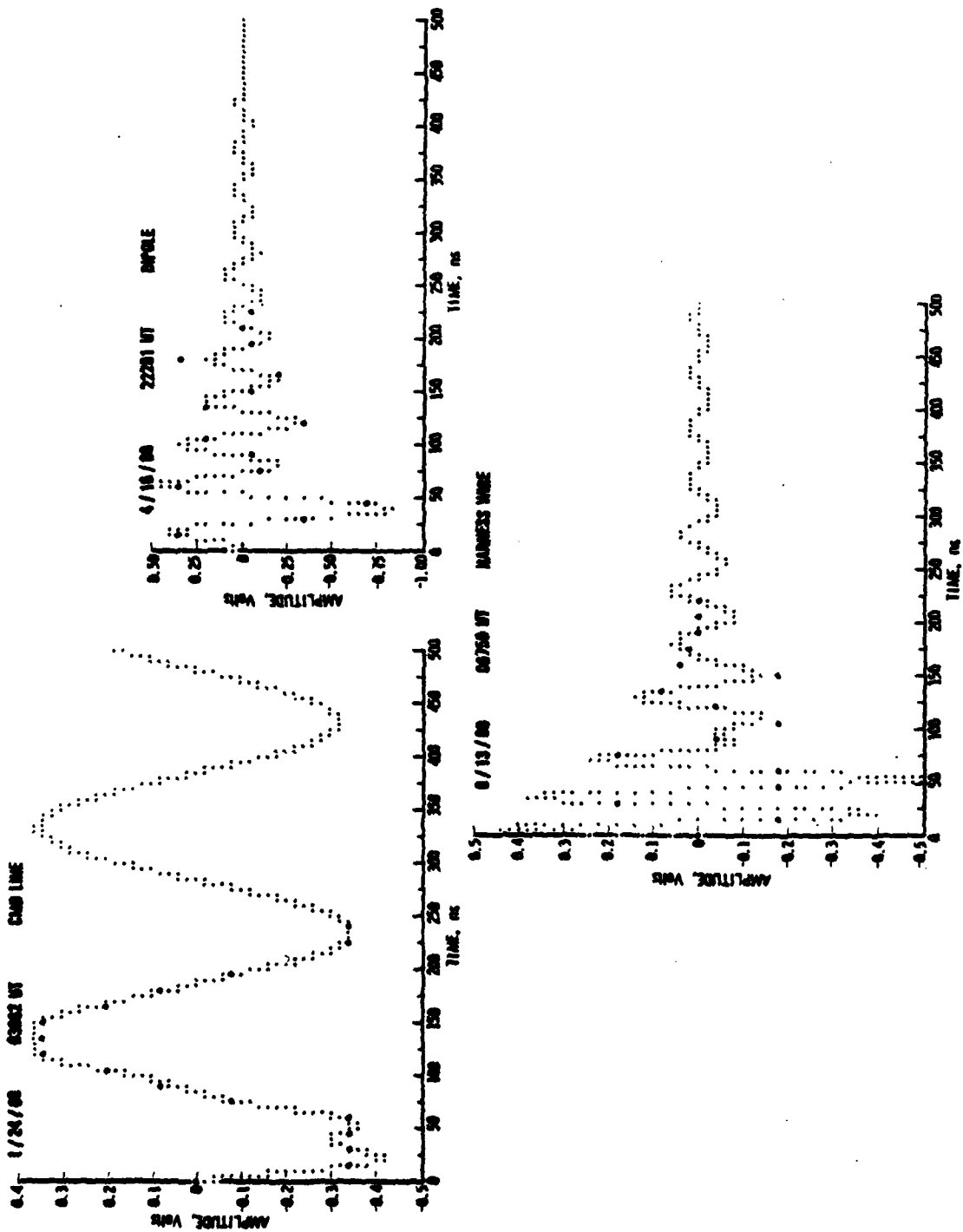


Figure 7. Shape of Three Natural Discharges Detected by the Pulse Analyzer. The large solid dots are the data points. The small dots are the result of a computed fit to the data points.

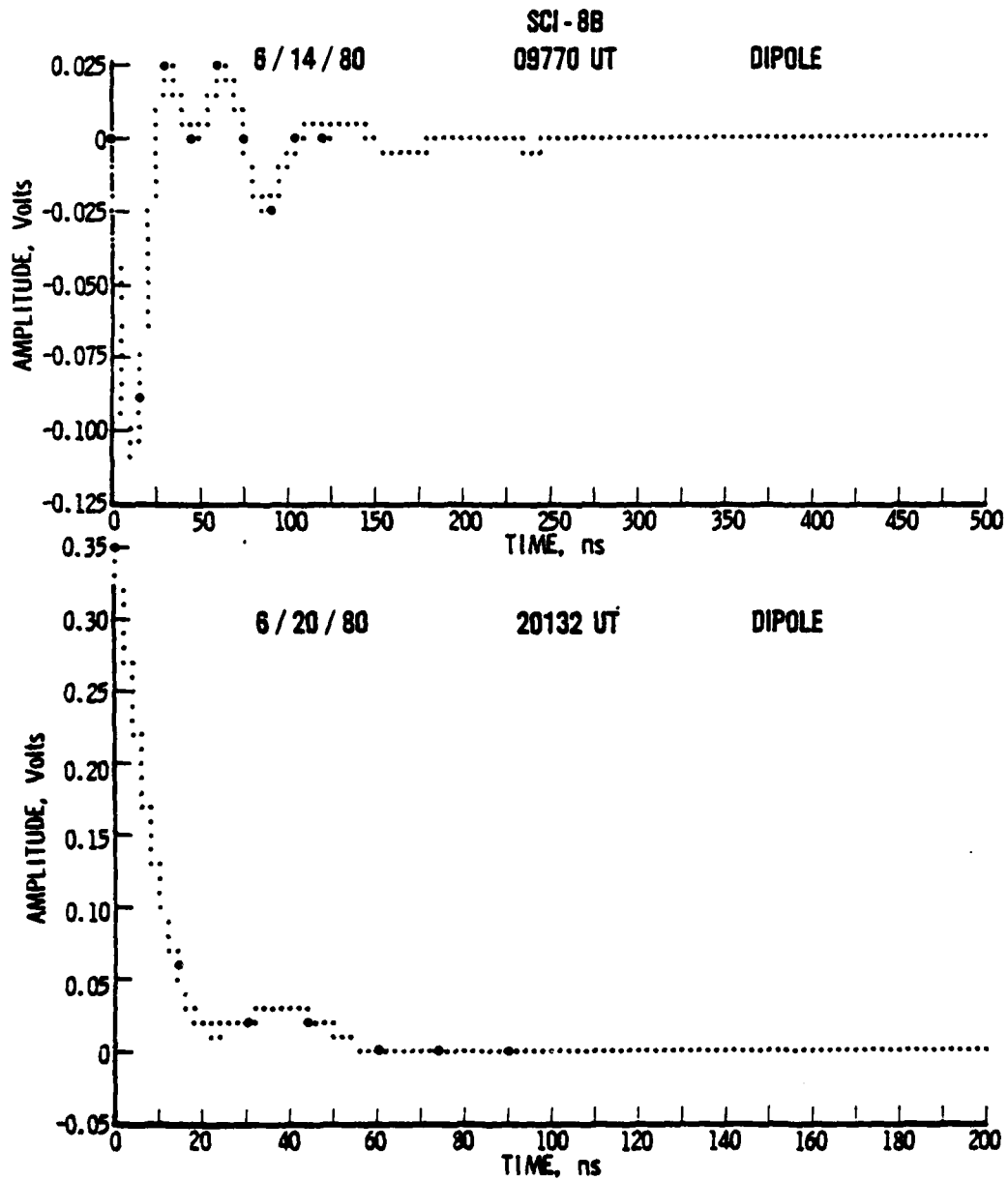


Figure 8. Shape of Two Natural Discharges Detected by the Pulse Analyzer. The large solid dots are the data points. The small dots are the result of a computed fit to the data points.

Table 6
PULSE FITTING PARAMETERS

DATE	UT		Sensor	i	Frequency		Amplitude		Damping		Phase	
	Seconds				MHz	volts	ns ⁻¹	deg				
ELECTRON GUN PULSE												
3/23/80	51096	CMD Line	0 1 2		14.1 26.4		-0.003	+3.57 x 10 ⁻³ -1.32 x 10 ⁻³	182.4 46.9			
							0.089					
							0.140					
VLF ANTENNA PULSE												
3/23/80	51860	CMD Line	0 1 2		9.0 16.0		-0.007	3.67 x 10 ⁻² 3.95 x 10 ⁻³	45.6 227.3			
							0.397					
							0.135					

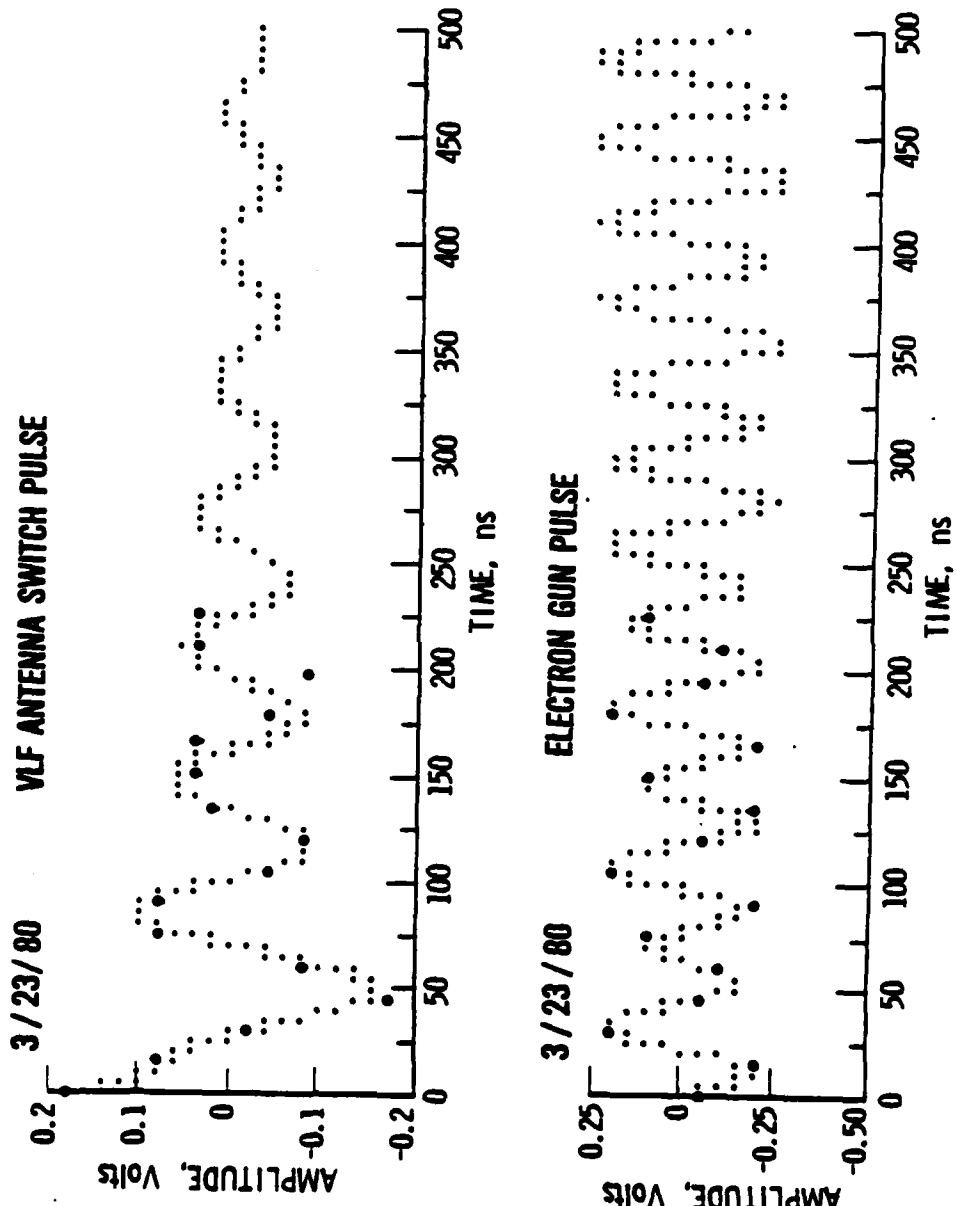


Figure 9. Shape of Two Pulses Due to Vehicle Operations. The large solid dots are the data points. The small dots are the result of a computed fit to the data points.

REFERENCES

1. Stevens, J. R., and Vampola, A. L.: Description of the Space Test Program P78-2 Spacecraft and Payloads, SAMSO TR-78-24, 1978.
2. McPherson, D. A.; Cauffman, D. P.; and Schober, W. R.: Spacecraft Charging at High Altitudes: SCATHA Satellite Program, J. Spacecraft and Rockets, Vol. 12, No. 10, Oct. 1975, pp. 621-626.

LABORATORY OPERATIONS

The Laboratory Operations of The Aerospace Corporation is conducting experimental and theoretical investigations necessary for the evaluation and application of scientific advances to new military space systems. Versatility and flexibility have been developed to a high degree by the laboratory personnel in dealing with the many problems encountered in the nation's rapidly developing space systems. Expertise in the latest scientific developments is vital to the accomplishment of tasks related to these problems. The laboratories that contribute to this research are:

Aerophysics Laboratory: Launch vehicle and reentry aerodynamics and heat transfer, propulsion chemistry and fluid mechanics, structural mechanics, flight dynamics; high-temperature thermomechanics, gas kinetics and radiation; research in environmental chemistry and contamination; cw and pulsed chemical laser development including chemical kinetics, spectroscopy, optical resonators and beam pointing, atmospheric propagation, laser effects and countermeasures.

Chemistry and Physics Laboratory: Atmospheric chemical reactions, atmospheric optics, light scattering, state-specific chemical reactions and radiation transport in rocket plumes, applied laser spectroscopy, laser chemistry, battery electrochemistry, space vacuum and radiation effects on materials, lubrication and surface phenomena, thermionic emission, photosensitive materials and detectors, atomic frequency standards, and bioenvironmental research and monitoring.

Electronics Research Laboratory: Microelectronics, GaAs low-noise and power devices, semiconductor lasers, electromagnetic and optical propagation phenomena, quantum electronics, laser communications, lidar, and electro-optics; communication sciences, applied electronics, semiconductor crystal and device physics, radiometric imaging; millimeter-wave and microwave technology.

Information Sciences Research Office: Program verification, program translation, performance-sensitive system design, distributed architectures for spaceborne computers, fault-tolerant computer systems, artificial intelligence, and microelectronics applications.

Materials Sciences Laboratory: Development of new materials: metal matrix composites, polymers, and new forms of carbon; component failure analysis and reliability; fracture mechanics and stress corrosion; evaluation of materials in space environment; materials performance in space transportation systems; analysis of systems vulnerability and survivability in enemy-induced environments.

Space Sciences Laboratory: Atmospheric and ionospheric physics, radiation from the atmosphere, density and composition of the upper atmosphere, aurorae and airglow; magnetospheric physics, cosmic rays, generation and propagation of plasma waves in the magnetosphere; solar physics, infrared astronomy; the effects of nuclear explosions, magnetic storms, and solar activity on the earth's atmosphere, ionosphere, and magnetosphere; the effects of optical, electromagnetic, and particulate radiations in space on space systems.

. . .

DATE
ILME
— 88